PROCEEDINGS OF SCIENCE

Galactic Cosmic Ray Observations with the High Energy Particle Detector (HEPD-01) on board the CSES-01 Satellite

Alessandro Sotgiu[a,*] **and Beatrice Panico**[b,c] **on behalf of the CSES-Limadou Collaboration**

(a complete list of authors can be found at the end of the proceedings)

[a] *National Institute of Nuclear Physics, section of Rome Tor Vergata, Via della Ricerca Scientifica, 1, Rome, Italy*

[b] *University of Naples "Federico II", Department of Physics, C.so Umberto I, 40, Naples, Italy*

[c] *National Institute of Nuclear Physics, section of Naples*

E-mail: alessandro.sotgiu@roma2.infn.it

The High-Energy Particle Detector (HEPD-01) is one of the payloads onboard the China Seismo-Electromagnetic Satellite (CSES-01), launched in February 2018 and still operating. The detector is a light and compact payload suitable for measuring electrons (3-100 MeV), protons (30-300 MeV), and light nuclei (up to a few hundred MeV/nucleon). The wide angular acceptance of HEPD-01, and the polar orbit of the satellite, allow for the measurement of galactic particle spectra also on a daily basis for protons. We present here some results concerning the measurement of galactic proton spectra between 40 and 250 MeV, together with a first preliminary measurement of galactic helium nuclei between 60 and 200 MeV/nucleon, obtained from the data collected in the first months of flight. The data-analysis techniques used to reconstruct helium fluxes are presented for the first time, and the clear particle separation of the two species inside the detector is shown. A comparison of HEPD-01 data with theoretical spectra obtained with Monte Carlo model is also presented. Proton-to-helium flux ratio at different energies is particularly important as the mass-to-charge ratio of the two particles is very different and it is a good probe for the study of cosmic-ray propagation and injection spectra.

38th International Cosmic Ray Conference (ICRC2023)
26 July - 3 August, 2023
Nagoya, Japan

*Speaker

PoS(ICRC2023)114

1. Introduction

Hydrogen nuclei, together with helium nuclei, account for almost 99% of the entire cosmic radiation, with the former being the most abundant component of charged galactic cosmic rays (GCRs) representing $\simeq$ 90% of the total CR budget. The acceleration of CRs, except for the highest energies, are believed to occur mainly in supernova remnants (SNRs) in the Galaxy, but unambiguous evidences have still to be found[1]. An important contribution at energies below few GeV is due to our Sun, which is not only a source of particles, but also has a significant effect on the propagation of cosmic rays in the heliosphere, modifying their energy spectra. This effect, called solar modulation, is the sum of a series of effects like convection, diffusion, adiabatic deceleration, and drift motions, all driven by the Heliospheric Magnetic Field (HMF) and with a strong time-dependent nature[2, 3]. The portion of the spectrum below a few hundred MeV is particularly interesting because the modulation effects are stronger and also because this range has been studied mostly by balloons and, more recently, by the PAMELA experiment[4, 5]. In this framework the HEPD-01 detector fits really well, extending the energy range of PAMELA at lower energies. In this work, we present some hydrogen and helium nucleai spectra measured by the High-Energy Particle Detector in the $\simeq 60MeV - 200MeV$ range.

2. The High-Energy Particle Detector 01

The High-Energy Particle Detector 01 (HEPD-01) is the Italian payload on board of the Chinese CAST2000-class satellite CSES-01. It is a compact payload (total mass ~45 kg) dedicated to the measurement of charged particle flux in the sub-GeV energy region. HEPD-01 is made up of the following subdetectors:

- a tracker, made of two planes of double-side silicon micro-strip sensors (21.3 cm $\times$ 21.5 cm $\times$ 0.03 cm), at the top of the instrument, to provide the particle trajectory;
- a trigger plane, which consists of one layer of plastic scintillator, divided into 6 segments (20 cm $\times$ 3 cm $\times$ 0.5 cm each). Together with different combinations of the calorimeter planes, it provides the trigger for the acquisition of charged events;
- a calorimeter, divided into 2 sections. The upper tower is composed of 16 plastic scintillators with dimensions 15 cm $\times$ 15 cm $\times$ 15 cm read out by two PMTs placed at opposite corners. The lower layer is made of a plane of 9 LYSO cubes, used to extend the energy range;
- a scintillator veto system, 4 lateral planes and a bottom one with a 5-mm thick, that surrounds the calorimeter, for particle containment and rejection of secondaries.

A more detailed description can be found in [6] and [7].

The CSES-01 satellite was launched on February 2, 2018 with an expected lifetime of ~5 years. It is placed in a 98° inclination Sun-synchronous circular orbit, at an altitude of ~500 km. The working zone was at the beginning in the latitude range [-65°,+65°], but after November 2019 it was changed to [-70°,+70°]. A scheme of the HEPD-01 detector and a picture of the instrument installed on board CSES-01 can be seen in Figure 1.

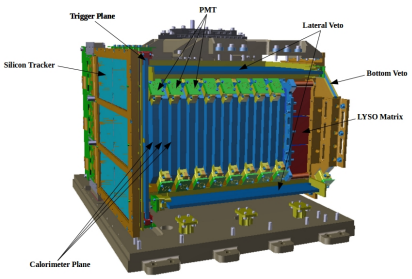

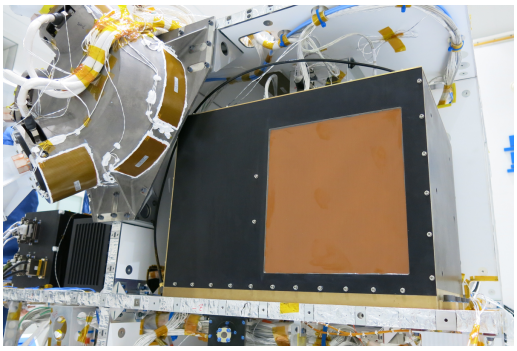

Figure 1: (Left) HEPD-01 detailed scheme including sensitive detectors and mechanical structures. (Right) A picture of HEPD-01 installed on board CSES-01.

3. Data analysis

3.1 Selection of proton and helium samples

The acquisition system of HEPD-01 includes eight predefined trigger configurations that can be changed according to the satellite's position along the orbit. The trigger configuration used for this analysis acquires the event if a signal above the threshold is registered in the trigger plane T1, together with the first and the second plane of the calorimeter tower (P1 & P2). Similar selections are used for the two particles. The criteria common to both particles are:

- the request that the signal of both PMTs of the same plane is above the threshold. All the scintillators in the HEPD-01 trigger planes are read by 2 PMTs. They contribute to the trigger if one of the PMTs collects a signal above the set threshold. The request that both PMTs of the same plane involved in the trigger mask are above the threshold is used offline to further clean the sample;
- fully containment inside the calorimeter (i.e. if one of the scintillators of the veto system is hit, the event is rejected). This is mandatory to guarantee that the entire energy of the primary particle is deposited inside the detector and correctly reconstructed;
- selection of galactic particles with a request on the L-shell parameter.

Concerning the last point, a simulation of all possible arrival directions of particles has been carried out, considering the instrument's field of view (FoV). A combination of the International Geomagnetic Field Reference (IGRF) model[8], AACGM (Altitude-Adjusted Geomagnetic Coordinates[9] and the Tsyganenko89 model[10] is adopted to take into consideration both internal and external magnetic field sources. As a result, a latitude/longitude static cutoff map is obtained and it has been verified that the condition of L-shell > 7 allows selecting region with a geomagnetic cutoff always below the energy threshold of the detector. Figure 2 shows the positions where galactic helium nuclei are selected according to this analysis and the corresponding energy cutoff value.

The live time calculation of the apparatus is performed via the trigger board. For consistency with the geographical criteria, the live time is accumulated only in polar regions where the energy

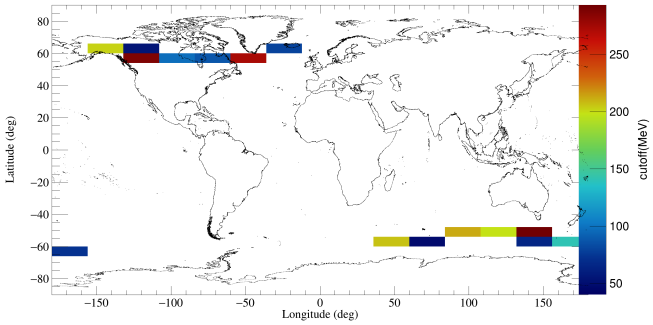

Figure 2: Geographical region selected with the condition of L-shell > 7 for He particles. It can be observed that the energy cutoff is always below 60 MeV/n that is the lower threshold used for this analysis.

cutoff is below the energy threshold of the HEPD-01 detector (e.g. the region in Figure 2 for He particles).

The discrimination between hydrogen nuclei and lepton populations and between helium nuclei and proton population is based on the signal deposited on the first scintillator plane (P1) as a function of the total deposited energy. For the proton selection, two curves are defined (quantiles at 15% and 95% for lower and upper curves, respectively) in order to define a selection band with a $\simeq$ 80% efficiency (see Figure 3, left). The helium selection is performed considering only a lower curve, as the contamination of heavier nuclei has been considered negligible (Figure 3, right). The efficiency of both selection criteria has been evaluated with an accurate Monte Carlo simulation that takes into account the scintillation light collection and efficiency and the electronics effect. Such simulation has been performed using the official software developed by the Limadou Collaboration, based on a GEANT4 toolkit[11], and has been carried out both for protons and helium nuclei. The energy range of the simulation is from $10 MeV/n$ to $40 GeV/n$ and the particles are generated within a large generation surface with an isotropic distribution ($0° < \theta < 90°$; $0° < \phi < 180°$, where θ and ϕ are the zenith and azimuth angles, respectively). For the helium simulation, only ^4He isotope has been considered in this analysis. Future optimizations that include also a ^3He component are planned.

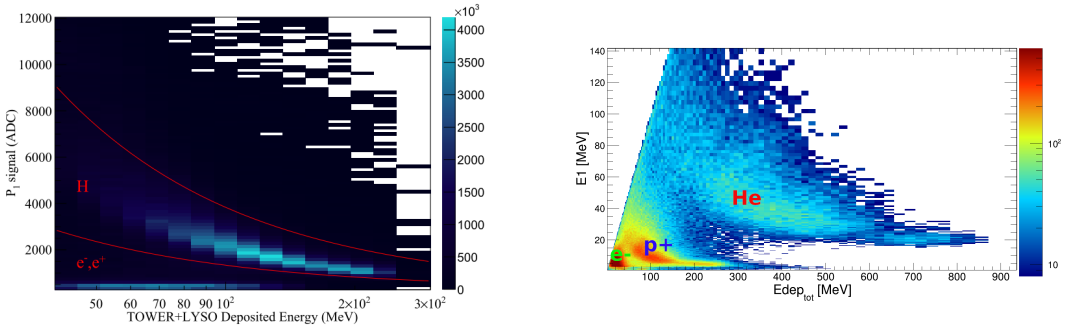

Figure 3: (Left) ADC signal on the first plane vs the total energy deposited into the calorimeter is showed. The red curves are used to select the proton population. (Right) The deposited energy on the first plane vs the total energy deposited into the calorimeter. The three population of electrons, protons and He nuclei are visible.

The same simulation has been used to evaluate the geometrical factor of HEPD-01, which is defined by the requirement of containment within the volume of the instrument. The total geometrical acceptance of HEPD-01 for Z=1 and Z=2 particles is shown in Figure 4. It can be noted that the shape is very similar for the two particles, with a strong energy dependence and a peak at $\simeq 90 MeV/n$ where it reaches the huge value of $\simeq 400 cm^2 sr$. There is a rapid decrease at lower energy, due to the energy threshold for particle detection, and a similar decrease at higher energies, due to the requirement of full containment. Various spectral shapes and energy ranges were used to cross-check the total acceptance as a function of the primary particle energy, and it was found constant within statistical errors.

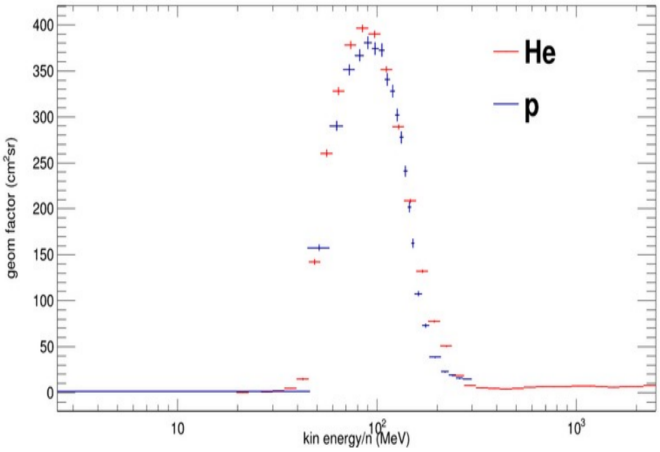

Figure 4: Geometrical factor of HEPD-01 for hydrogen and helium nuclei as a function of the energy of the primary particle.

3.2 Unfolding and flux calculation

The energy measured by means of the HEPD-01 calorimeter must be corrected to account for particle slow-down and energy loss in the passive material of the mechanical structures covering the sensitive materials of the apparatus. The correction has been applied by means of an unfolding procedure, following the classical Bayesian approach[12]. The detector response matrix, or smearing matrix, has been obtained from dedicated proton and helium simulations, with a generic cosmic-ray spectrum (modulated power law) as an input. Once the primary energy has been correctly reconstructed, it is possible to obtain the differential fluxes starting from the observed counts and considering the geometric factor, the live time, and the detector efficiencies obtained through simulations. Contamination in the particle samples has been also evaluated using Monte Carlo simulations and treated as systematic uncertainties.

4. Results

A semi-annual galactic hydrogen and helium spectra as a function of energy between 60 and 200 MeV/n has been obtained for the period August 2018 - January 2019 and compared to the theoretical prediction from the HelMod model[13] in the same period. A more detailed discussion

on the proton results achieved by HEPD-01 can be found in [14] and [15] or during the presentation, together with the first results of the helium analysis.

References

[1] Mirko Boezio, Riccardo Munini, and Piergiorgio Picozza. "Cosmic ray detection in space". In: *Progress in Particle and Nuclear Physics* 112 (2020), p. 103765. ISSN: 0146-6410. DOI: https://doi.org/10.1016/j.ppnp.2020.103765. URL: https://www.sciencedirect.com/science/article/pii/S0146641020300120.

[2] M.D. Ngobeni et al. "Simulations of the solar modulation of Helium isotopes constrained by observations". In: *Advances in Space Research* 69.5 (2022), pp. 2330–2341. ISSN: 0273-1177. DOI: https://doi.org/10.1016/j.asr.2021.12.018. URL: https://www.sciencedirect.com/science/article/pii/S0273117721009285.

[3] M.S. Potgieter. "The global modulation of cosmic rays during a quiet heliosphere: A modeling perspective". In: *Advances in Space Research* 60.4 (2017). Solar Energetic Particles, Solar Modulation and Space Radiation: New Opportunities in the AMS-02 Era, pp. 848–864. ISSN: 0273-1177. DOI: https://doi.org/10.1016/j.asr.2016.09.003. URL: https://www.sciencedirect.com/science/article/pii/S0273117716304999.

[4] O. Adriani et al. "PAMELA Measurements of Cosmic-Ray Proton and Helium Spectra". In: *Science* 332.6025 (Apr. 2011), p. 69. DOI: 10.1126/science.1199172. arXiv: 1103.4055 [astro-ph.HE].

[5] M. Martucci et al. "Proton Fluxes Measured by the PAMELA Experiment from the Minimum to the Maximum Solar Activity for Solar Cycle 24". In: *The Astrophysical Journal Letters* 854.1 (Feb. 2018), p. L2. DOI: 10.3847/2041-8213/aaa9b2. URL: https://dx.doi.org/10.3847/2041-8213/aaa9b2.

[6] G. Ambrosi et al. "Beam test calibrations of the HEPD detector on board the China Seismo-Electromagnetic Satellite". In: *Nuclear Instruments and Methods in Physics Research A* 974, 164170 (Sept. 2020), p. 164170. DOI: 10.1016/j.nima.2020.164170.

[7] G. Ambrosi et al. "The electronics of the High-Energy Particle Detector on board the CSES-01 satellite". In: *Nuclear Instruments and Methods in Physics Research A* 1013, 165639 (Oct. 2021). DOI: 10.1016/j.nima.2021.165639.

[8] E. Thébault, CC. Finlay, and H. Toh. "Special issue International Geomagnetic Reference Field—the twelfth generation". In: *Earth, Planets and Space* 67 (Sept. 2015). DOI: 10.1186/s40623-015-0313-0.

[9] S.G. Shepherd. "Altitude-adjusted corrected geomagnetic coordinates: Definition and functional approximations". In: *JGR: Space Physics* 119 (Aug. 2014). DOI: https://doi.org/10.1002/2014JA020264.

[10] N.A. Tsyganenko. "A magnetospheric magnetic field model with a warped tail current sheet". In: *Planetary and Space Science* 37.1 (1989), pp. 5–20. ISSN: 0032-0633. DOI: https://doi.org/10.1016/0032-0633(89)90066-4. URL: https://www.sciencedirect.com/science/article/pii/0032063389900664.

[11] S. Agostinelli et al. "G EANT4—a simulation toolkit". In: *Nuclear Instruments and Methods in Physics Research A* 506.3 (July 2003), pp. 250–303. DOI: 10.1016/S0168-9002(03)01368-8.

[12] G. D'Agostini. "A multidimensional unfolding method based on Bayes' theorem". In: *Nuclear Instruments and Methods in Physics Research Section A: Accelerators, Spectrometers, Detectors and Associated Equipment* 362.2 (1995), pp. 487–498. ISSN: 0168-9002. DOI: https://doi.org/10.1016/0168-9002(95)00274-X. URL: https://www.sciencedirect.com/science/article/pii/016890029500274X.

[13] M.J. Boschini et al. "The HelMod model in the works for inner and outer heliosphere: From AMS to Voyager probes observations". In: *Advances in Space Research* 64.12 (2019). Advances in Cosmic-Ray Astrophysics and Related Areas, pp. 2459–2476. ISSN: 0273-1177. DOI: https://doi.org/10.1016/j.asr.2019.04.007. URL: https://www.sciencedirect.com/science/article/pii/S0273117719302509.

[14] S. Bartocci et al. "Galactic Cosmic-Ray Hydrogen Spectra in the 40-250 MeV Range Measured by the High-energy Particle Detector (HEPD) on board the CSES-01 Satellite between 2018 and 2020". In: *The Astrophysical Journal* 901.1, 8 (Sept. 2020), p. 8. DOI: 10.3847/1538-4357/abad3e.

[15] M. Martucci et al. "Time Dependence of 50–250 MeV Galactic Cosmic-Ray Protons between Solar Cycles 24 and 25, Measured by the High-energy Particle Detector on board the CSES-01 Satellite". In: *The Astrophysical Journal Letters* 945.2 (Mar. 2023), p. L39. DOI: 10.3847/2041-8213/acbea7. URL: https://dx.doi.org/10.3847/2041-8213/acbea7.

Full Authors List: CSES-Limadou Collaboration

S. Bartocci[a], R. Battiston[b,c], W. J. Burger[c], D. Campana[d], G. Castellini[e], P. Cipollone[a], L. Conti[f,a], A. Contin[g,h], C. De Donato[a], C. De Santis[a], F. M. Follega[b,c], G. Gebbia[b,c], R. Iuppa[b,c], M. Lolli[h], M. Martucci[a], G. Masciantonio[a], M. Mergè[i,a], M. Mese[l,d], C. Neubüser[c], F. Nozzoli[c], A. Oliva[h], G. Osteria[d], L. Pacini[m], F. Palma[a], F. Palmonari[g,h], B. Panico[l,d], F. Perfetto[d], P. Picozza[n,a], M. Pozzato[h], E. Ricci[b,c], M. Ricci[o], S. B. Ricciarini[e], Z. Sahnoun[g,h], V. Scotti[l,d], A. Sotgiu[a], R. Sparvoli[n,a], V. Vitale[a], S. Zoffoli[i] and P. Zuccon[b,c]

[a] INFN-Sezione di Roma "Tor Vergata", Via della Ricerca Scientifica 1, I-00133 Roma, Italy
[b] University of Trento, Via Sommarive 14, I-38123 Povo (Trento), Italy
[c] INFN-TIFPA, Via Sommarive 14, I-38123 Povo (Trento), Italy
[d] INFN-Sezione di Napoli, Via Cintia, I-80126 Napoli, Italy
[e] IFAC-CNR, Via Madonna del Piano 10, I-50019 Sesto Fiorentino (Firenze), Italy
[f] Uninettuno University, Corso V. Emanuele II 39, I-00186 Roma, Italy
[g] University of Bologna, Viale Berti Pichat 6/2, Bologna, Italy
[h] INFN-Sezione di Bologna, Viale Berti Pichat 6/2, Bologna, Italy
[i] Italian Space Agency, Via del Politecnico, I-00133 Roma, Italy
[l] University of Napoli "Federico II", Via Cintia, I-80126 Napoli, Italy
[m] INFN-Sezione di Firenze, Via Sansone 1, I-50019 Sesto Fiorentino (Firenze), Italy
[n] University of Roma "Tor Vergata", Via della Ricerca Scientifica 1, I-00133 Roma, Italy
[o] INFN-LNF, Via E. Fermi 54, I-00044 Frascati (Roma), Italy

PoS(ICRC2023)114